Electronic Supplementary Material (ESI) for Lab on a Chip.


Supporting Information

# A microscopy-compatible temperature regulation system for single-cell phenotype analysis – demonstrated by thermoresponse mapping of microalgae

Martin Andersson, Sofia Johansson, Henrik Bergman, Linhong Xiao, Lars Behrendt and Maria Tenje

Dr. M. Andersson, Dr. S. Johansson, H. Bergman, and Prof. M. Tenje

Dept. Materials Science and Engineering, Science for Life Laboratory, Uppsala University, Box 35, 751 03 Uppsala, Sweden.

E-mail: maria.tenje@angstrom.uu.se

Dr. L. Xiao and Dr. L. Behrendt

Dept. Organismal Biology, Science for Life Laboratory, Uppsala University, Norbyvägen 18A, 752 36 Uppsala, Sweden

E-mail: lars.behrendt@scilifelab.uu.se

**Supplementary Information 1: Description of calibration procedure.**

To calibrate the RTDs T1-T6, a reference Pt-100 temperature sensor (IEC751 Class A, 666-7359 RS PRO) was used. The reference sensor was connected to a multimeter (2015, Keithley) in a 4-point configuration. The reference sensor was mounted on a 7 x 5 $mm^2$ polished slab of AlN by thermal paste and epoxy glue, and then embedded in a 7 mm high and 25 mm wide PDMS slab. This PDMS/AlN reference device was then mounted onto the heat stage, with the AlN slab aligned directly over T1-T6 and a thin film of oil for good thermal contact. The high thermal conductance of the AlN slab ensured that the temperature remained uniform across the thermally regulated window with the array of RTDs and the Pt-100. The PDMS provided thermal isolation. The heat-stage and AlN slab was first heated up using H1-H6 to 50˚C (as determined by the Pt-100 reference). Sequentially, heating was turned off and logging of the reference temperature as well as the resistance of T1-16 was started. By cooling to ambient temperature, a temperature range between 22 – 50 ˚C was covered. Coefficients for the relationship between resistance and temperature were found for each temperature sensor using linear fitting to the following relationship

$$R_{RTD}(T)=R_{nom}(1+\alpha T) \quad \text{(S1)}$$

where $R_{RTD}$ is the resistance measured with the temperature sensor and $T$ is the temperature. The temperature coefficient, $\alpha$, is considered to be temperature independent in the considered temperature interval.

**Supplementary Information 2: Operation in manual mode.**

This section discusses the temperature response of the Joule heaters to a change in the applied power and evaluates the effects of the external environment, such as cooling flow and adding a PDMS/AlN chip on the heat-stage.

First, the steady-state temperature, $T_{eq}$, at a power of 300 mW applied to each heater was evaluated. As power is applied to the heaters, the temperature increases and stabilizes at each heater's individual steady-state temperature as shown in Figure S1A-B. The differences in steady-state temperature observed between the six heaters on the heat-stage is attributed to two main reasons: The resistance varies somewhat from one heater to another with typical values of 65-70 Ω and the heaters closest to the edges carries a larger thermal load than those in the center of the array, as they heat up a larger amount of glass and cooling liquid.

Placing a PDMS/AlN reference chip on the heat-stage or varying the flow of cooling liquid affects the steady-state temperature. In Figure S1C the decrease of the steady-state temperature with increasing cooling flow is plotted for one heater. It should be noted that the cooling liquid itself warms up when passing the heaters, thus causing more cooling at the inlet compared to the outlet of the channel. This is causing a natural temperature gradient across the array of heaters with the lowest temperature closest to inlet of the cooling liquid and the highest temperature closest to the outlet.

Time constants and sensitivity were calculated to further analyze the inherent performance of the heat-stage. To find the time constant, $\tau$, the temperature response, $T(t)$, as the power is switched on can be modelled as a first order system.

$$T(t) = T_{eq}\left(1 - e^{-t/\tau}\right) \qquad \text{(S2)}$$

An analogous expression is used to find the time constants when switching the power OFF. The time constants of the heat-stage presented in Figure S1D and show a decrease with increasing flow rate and an increase as the reference chip is placed on the stage. The sensitivity may be calculated as the applied power (300 mW) divided by the steady-state temperature. Both ends of the sensitivity range are well within the range of which the heat-stage is operated.

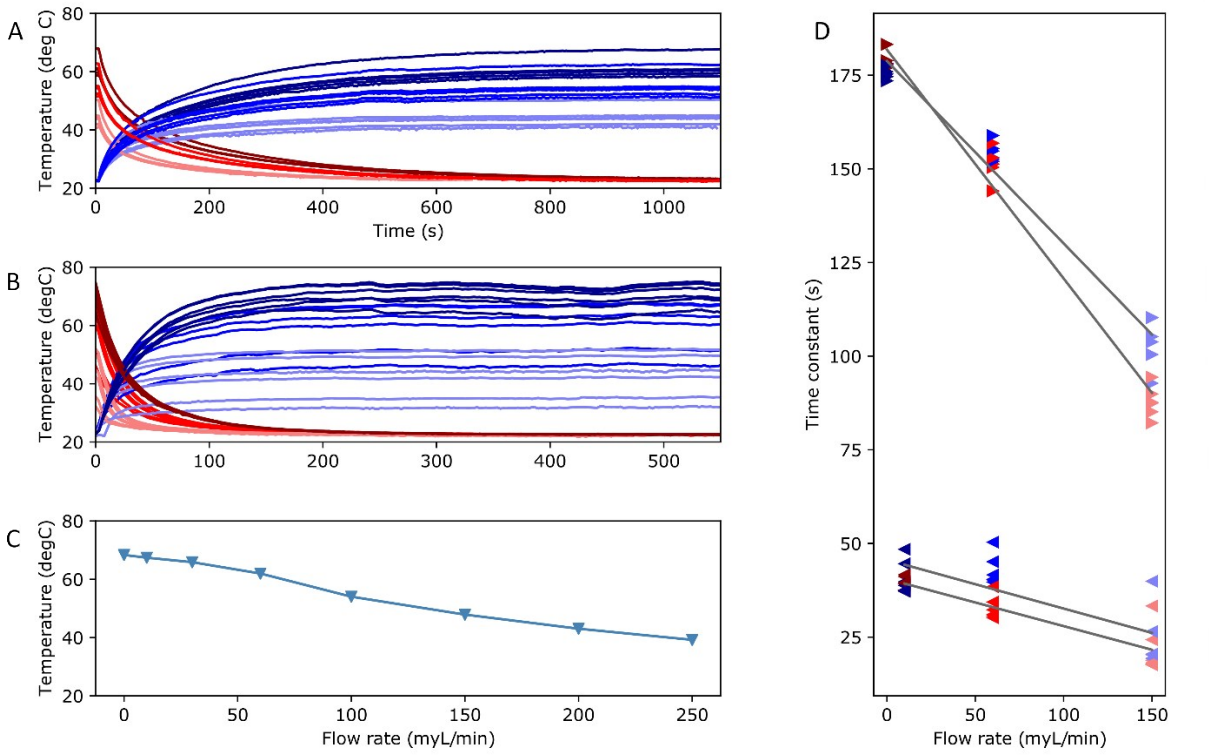


**Figure S1. Performance of heat stage operating in manual mode as a function of cooling flow rate.** (A), (B) Temperature of T1-T6 as a function of time. At *t*= 0 s, 300 mW power is either turned on (blue) or turned off (red) for each heater. Cooling flow rate was 0 (dark red/blue), 60 µl/min (clear red/blue) or 150 µl/min (light red/blue). Either the PDMS/AlN reference device was placed onto the heat stage (A) or no chip was placed on the heat stage (B). (C) The steady state temperature as a function of cooling flow rate was measured using the reference temperature sensor in the PDMS/AlN reference device. (D) The corresponding time constants of the response shown in (A) and (B) when turning ON or OFF the heaters as a function of cooling flow rate. Tests when the PDMS/AlN reference device was on the heat stage is indicated by right pointing (>) data points. Tests when the PDMS/AlN reference device was not placed on the heat-stage is indicated by left-pointing (<) data points. The grey lines shows linear fittings for time constants.

**Supplementary Information 3: Operation in automatic mode.**

The temperature regulation in automatic mode use the control function of the equation below where *P* and *I* are the proportional and integral coefficients, respectively, *u(t)* is the control variable and *e(t)* is the error.

$$u(t) = Pe(t) + I\int_0^t e(t')dt' \qquad \text{(S3)}$$

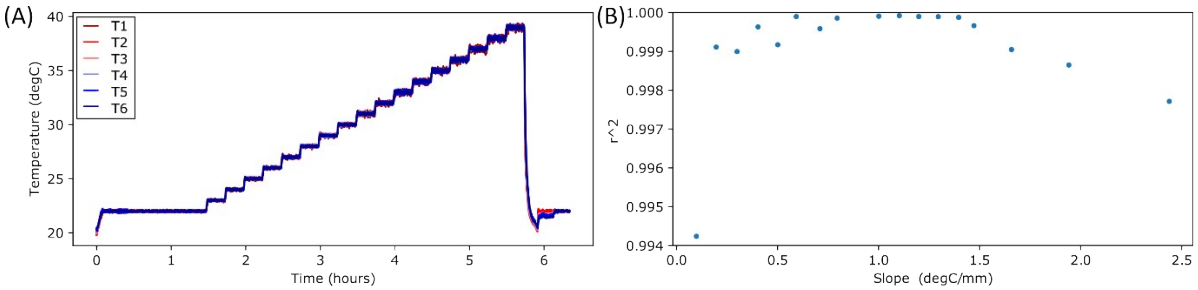


**Figure S2. Spatiotemporal profiles programmed in automatic mode.** (A) Stepwise increasing temperature are measured by the temperature sensors (T1-T6) as a function of time while controlling H1-H6 via the feedback system. Set-points were changed with a step-wise increase of 1°C every 15 min in the range 22-39°C. At *t*= 0 h, the heaters are turned ON and set to regulate at 22°C, at 1.5 h the step-wise profile is started and at *t*= 5.7 h, a set-point of 22°C is again applied. (B) The linearity of the spatial gradients in Figure 5A are assessed by the squared correlation coefficient ($r^2$) as a function of slope. Linear fittings to the measured temperatures were used to deduce the coefficients.

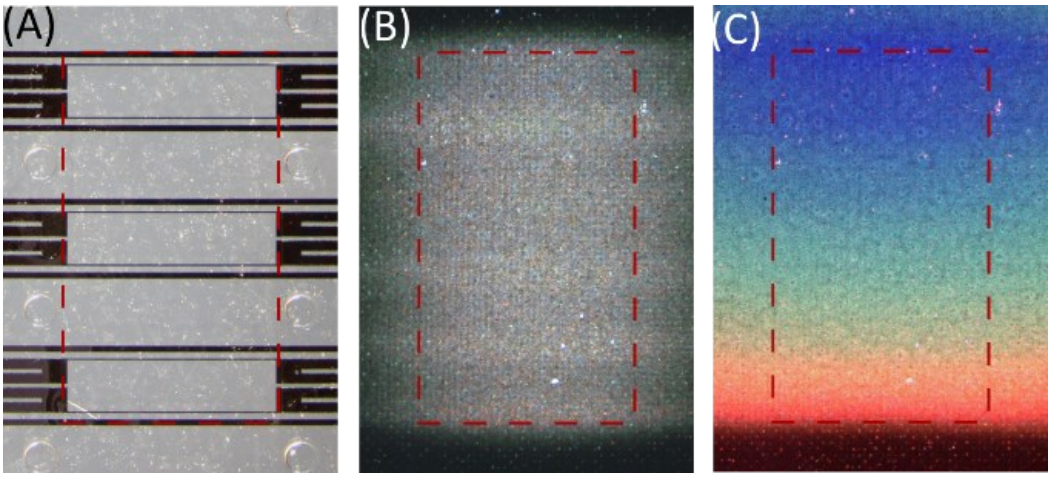


**Figure S3. Temperature distributions on the heat-stage visualized via a thermally responsive liquid crystal sheet**. (A) Brightfield image of the heat-stage with the temperature control window marked by red dashed lines. (B), (C) The same location as in (A) but with a thermally responsive liquid crystal sheet (cross-over temperature: 30°C) mounted onto a glass slide placed on the stage. (B) Constant temperature. No cooling flow was applied. (C) H1-H6 are set to form a thermal linear gradient with a

slope of 1.5°C/mm as regulated by the PI controllers and having H1 set to 30°C. A cooling flow was present (direction upwards in the image).

**Supplementary Information 4: Hardware used in temperature regulation system.**

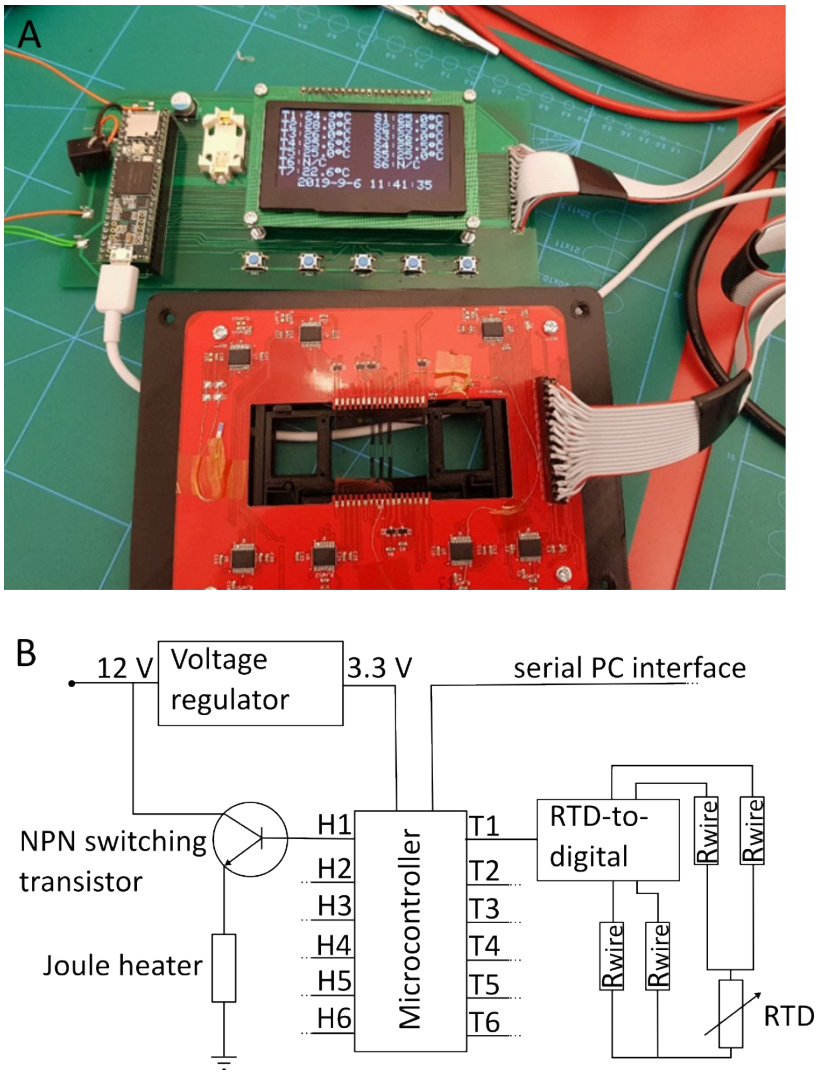


**Figure S4: Hardware of the temperature regulation system.** (A) A photograph of the assembled temperature regulation system. The upper green PCB is the temperature regulation unit, which includes the microcontroller and a display (not used in this study). The red PCB below connects to the glass heat-stage and is fitted on a 3D printed microscopy stage-insert. (B) A schematic circuit diagram indicating all key elements of the temperature regulation system. From top left: 12 V (DC) is applied and voltage regulated (LM1117) to 3.3V, a Teensy 3.6 microcontroller is powered by the 3.3 V and can communicate with a PC software using a serial interface. The microcontroller also sets the power, through pulse-width modulation, applied to the heaters (H1-H6). The power is switched ON and OFF on NPN switching transistors (PMBT3904), fed by 12 V and with the Joule heater connected between emitter and ground. The temperatures (T1-T6) are measured by the microcontroller through a RTD-to-digital converter (MAX31865) in a 4-point configuration. This in order to eliminate the resistance of the wires, Rwire. To avoid self-heating, the RTDs are run in 1-Shot mode i.e. bias is only applied when the temperatures are measured and not continuously. To simplify the figure, only one circuit leg is drawn for the heater and RTD, respectively.

**Supplementary Information 5: Microfluidic chip design.**

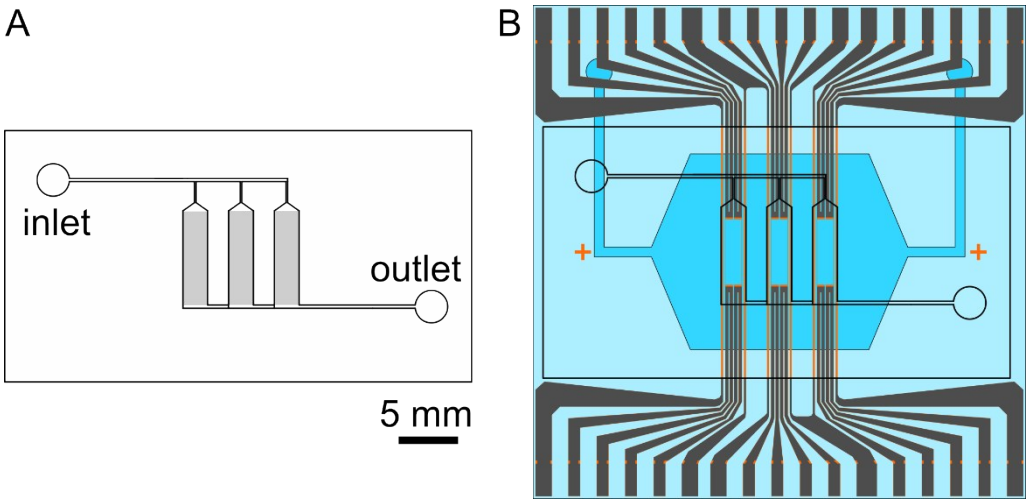


**Figure S5: Design of the PDMS/glass microfluidic chip used in this study and its alignment to the heat-stage.** (A) The microfluidic chip design contains three microwell arenas (marked in light grey), which branch out from a main microchannel (height: 75 µm). Each arena (1.53 mm × 5.75 mm) contains a total of 5.510 microwells (20-µm-diameter) spaced at 20 µm. (B) The design of the microfluidic chip is placed on top of the design of the heat-stage to illustrate the alignment of the microwell arenas with the heater/sensor electrodes and the active cooling channel of the heat-stage.

**Supplementary Information 6: Loading and immobilizing *Symbiodinium* CCMP2467 and CCMP421 into microfluidic geometries**

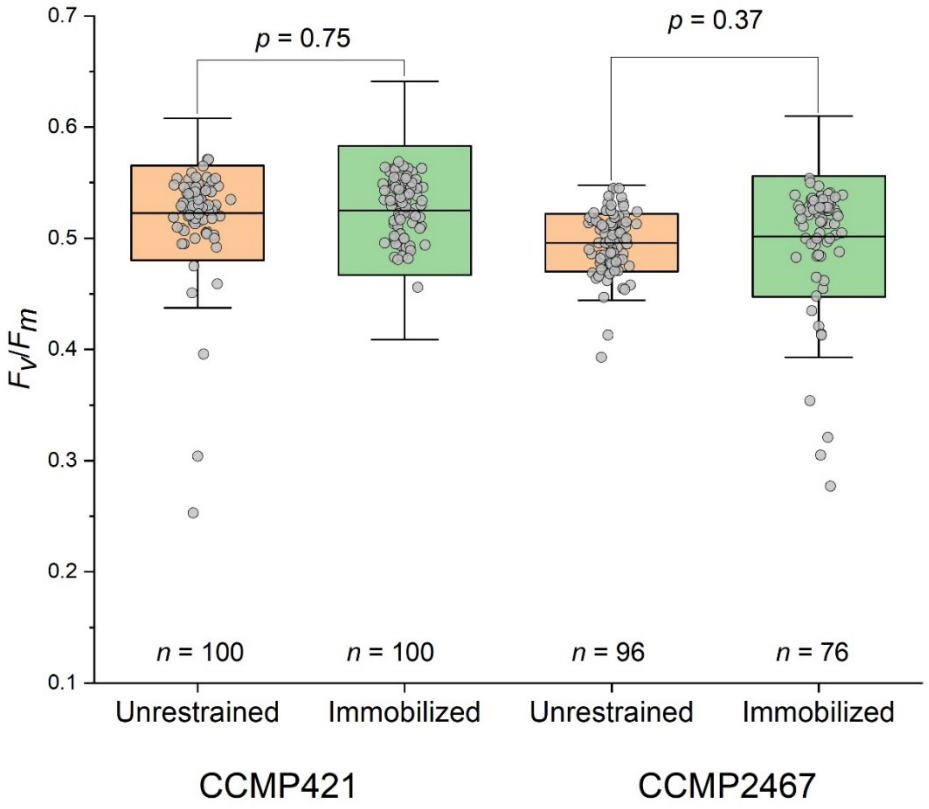


**Figure S6: Loading and immobilizing *Symbiodinium* CCMP2467 and CCMP421 into microfluidic geometries does not affect their photophysiology.** Comparison between dark-adapted maximum quantum yields ($F_v/F_m$) of unrestrained vs. immobilized cells of Symbiodinium strain CCMP421 and CCMP2467. All cells originated from the same culture. Unrestrained cells were imaged for their $F_v/F_m$ by placing them onto a microscopy slide within a sealing gasket (height 500 µm), whereas immobilized cells underwent the standard loading procedure used to immobilize cells (see Experimental section). Cells within microfluidic devices do not differ from unrestrained cells in $F_v/F_m$ ($p$ = 0.75 or $p$ = 0.37, two-sample t- test). Sample size ($n$) is indicated below box-and-whisker-plots, which display the mean (black line) and 1 (box heights) and 2 standard deviations (SD, whiskers).

**Supplementary Information 7: Short-term and long-term step-wise increasing temperatures applied to *Symbiodinium* CCMP2467 and CCMP421 and the reduction of avarage $F_v/F_m$ in percentage**.

**Table S1. Reduction of average $F_v/F_m$ for *Symbiodinium* CCMP2467 and CCMP421 during thermal stress.** Cells were exposed to either short-term temperature exposure or long-term temperature exposure. During short term temperature exposures the temperature was increased by +1°C every 15 min ($F_v/F_m$ assessed every 5 min), while during long-term temperature exposures the temperature was increased by +1°C every 6 h ($F_v/F_m$ assessed every 15 min). Reduction in the average $F_v/F_m$ was calculated by comparing the initial $F_v/F_m$ (at 22 ˚C) to the average $F_v/F_m$ at a given temperature. The threshold for detecting $F_v/F_m$ was 0.05 and values below this threshold are marked in red.

| | *Short-term* | | | | *Long-term* | | | |
|---|---|---|---|---|---|---|---|---|
| | **CCMP421** | | **CCMP2467** | | **CCMP421** | | **CCMP2467** | |
| Temp. [˚C] | Average $F_v/F_m$ ± SD | % reduction | Average $F_v/F_m$ ± SD | % reduction | Average $F_v/F_m$ ± SD | % reduction | Average $F_v/F_m$ ± SD | % reduction |
| 22.00 | **0.38** ± 0.04 | 0 | **0.39** ± 0.01 | 0 | **0.35** ± 0.01 | 0 | **0.43** ± 0.00 | 0 |
| 23.00 | **0.38** ± 0.00 | -0.51 | **0.39** ± 0.00 | 0.44 | **0.34** ± 0.00 | 2.71 | **0.43** ± 0.00 | 0.21 |
| 24.00 | **0.39** ± 0.00 | -1.98 | **0.38** ± 0.00 | 3.54 | - | | **0.40** ± 0.01 | 5.78 |
| 25.00 | **0.40** ± 0.00 | -3.19 | **0.37** ± 0.00 | 5.41 | **0.36** ± 0.00 | -2.24 | **0.37** ± 0.00 | 13.88 |
| 26.00 | **0.38** ± 0.00 | 1.40 | **0.36** ± 0.00 | 8.51 | **0.35** ± 0.00 | -1.26 | **0.34** ± 0.00 | 20.36 |
| 27.00 | **0.36** ± 0.00 | 4.73 | **0.34** ± 0.00 | 13.64 | **0.33** ± 0.00 | 6.42 | **0.30** ± 0.01 | 29.92 |
| 28.00 | **0.35** ± 0.00 | 7.28 | **0.31** ± 0.00 | 21.27 | **0.33** ± 0.00 | 6.71 | **0.25** ± 0.01 | 40.47 |
| 29.00 | **0.35** ± 0.00 | 8.98 | **0.28** ± 0.01 | 29.55 | **0.33** ± 0.00 | 6.11 | **0.19** ± 0.02 | 54.20 |
| 30.00 | **0.34** ± 0.00 | 10.81 | **0.21** ± 0.03 | 45.17 | **0.32** ± 0.00 | 9.16 | **0.12** 0.02 | 71.62 |
| 31.00 | **0.33** ± 0.00 | 12.60 | **0.16** ± 0.02 | 59.79 | **0.31** ± 0.00 | 12.53 | **0.06** ± 0.01 | 85.80 |
| 32.00 | **0.32** ± 0.00 | 15.12 | **0.10** ± 0.01 | 74.50 | **0.27** ± 0.01 | 22.66 | **0.02** ± 0.00 | 95.08 |
| 33.00 | **0.31** ± 0.00 | 18.30 | **0.03** ± 0.00 | 90.88 | **0.23** ± 0.01 | 33.51 | **0.00** ± 0.00 | 97.95 |
| 34.00 | - | - | - | - | **0.17** ± 0.03 | 51.35 | - | - |
| 35.00 | - | - | - | - | **0.04** ± 0.02 | 88.28 | - | - |
| 36.00 | - | - | - | - | **0.00** ± 0.00 | 98.23 | - | - |

**Supplementary Information 8: Sine single-cell response**

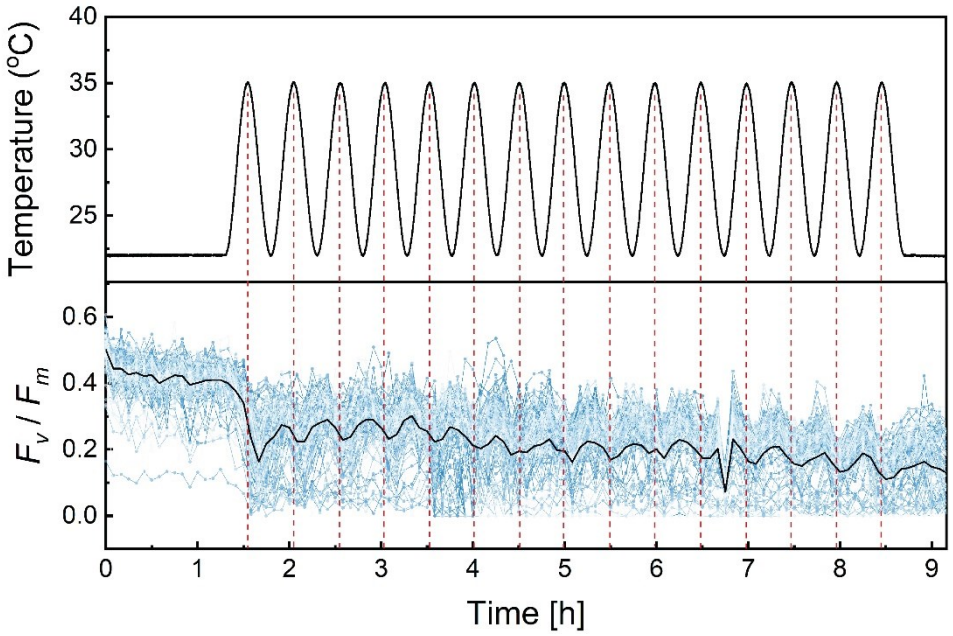


**Figure S7: Sinusoidal temperature profiles cause progressively declining $F_v/F_m$ in *Symbiodinium* CCMP2467.** Single-cell maximum quantum yields ($F_v/F_m$, $n$ = 133) under application of a sinusoidal temperature profile oscillating from 22°C to 35°C with a period of 30 min. Black lines shows the running average of all cells (no SD shown). At $t$= 0 h, the heaters are turned on and set to regulate at 22°C. At t= 1 h 20 min, the oscillating profile is started. At $t$=7 h 20 min, temperatures are set back to 22°C. During the entire experiment $F_v/F_m$ was assessed every 5 min and cells were otherwise kept in the dark.